International Journal of Science and Research Archive
eISSN: 2582-8185
Cross Ref DOI: 10.30574/ijsra
Journal homepage: https://ijsra.net/

(Research Article)

Combustion characteristics of a spark ignition engine fueled by high proportion ethanol-gasoline blends: A simulation approach

Trung Thuc Do [1, 2], Yong Tang [1], Trinh Xuan Phong [3] and Khanh Nguyen Duc [4, *]

[1] *School of Mechanical and Automotive Engineering, South China University of Technology, Guangzhou, 510640, China.*
[2] *Vietnam National University of Agriculture, Hanoi, 10000, Vietnam.*
[3] *Nam Dinh University of Technology Education, Nam Dinh 420000, Vietnam.*
[4] *School of Mechanical Engineering, Hanoi University of Science and Technology, Hanoi, 10000, Vietnam.*

International Journal of Science and Research Archive, 2025, 15(01), 127-142

Publication history: Received on 14 February 2025; revised on 31 March 2025; accepted on 02 April 2025

Article DOI: https://doi.org/10.30574/ijsra.2025.15.1.0934

Abstract

This research aims to find the effects of ethanol-gasoline blends on the combustion process of an automobile engine by a simulation approach. A comprehensive simulation model was developed based on dedicated AVL Boost and to be validated by experiment data. The engine model was controlled to operate with different ethanol-gasoline blends. In addition, the use of HHO as an additional supplement in the intake system was considered as a solution for the engine's technical performance and combustion process. The simulation process was carried out with various ethanol blending ratios ranging from E100 to E50, as well as conventional gasoline. HHO was introduced into the intake manifold as an additive at a ratio of 0.1% by volume the intake air, with the aim of improving the combustion quality in engines using ethanol-gasoline blends. Combustion characteristics such as in-cylinder pressure, temperature, heat release rate (RoHR), and Mass Fraction Burned (MFB) were analyzed and evaluated across different fuel scenarios. The simulation results showed that for high ethanol blends (from E70 to E100), the combustion process tended to be slower, as indicated by a decrease in peak pressure, peak temperature, and RoHR. In contrast, the E50 blend yielded better performance, with improvements in all these indicators. When HHO was added to the intake as an additive, it enhanced the combustion process, reflected in increased pressure, temperature, and RoHR. The impact of HHO became more pronounced with higher ethanol content in the fuel, especially in the E100 blend.

Keywords: Bio-Ethanol; Bi-Fuel Ethanol; HHO; Hydroxide

1. Introduction

Extensive research, both theoretical and experimental, has been conducted worldwide to assess bio-ethanol as an alternative fuel for internal combustion engines. The results have been noteworthy, offering valuable insights that support the broader adoption of bio-ethanol and the development of sustainable and eco-friendly energy solutions. Various studies have demonstrated the application of bio-ethanol in spark ignition (S.I.) engines, either as a standalone fuel or as part of blended mixtures [1]. Additionally, it has been incorporated into compression ignition (C.I.) engines when combined with other fuels [2]. Prior research has provided comprehensive explanations regarding bio-ethanol's characteristics and how they influence engine functionality [3].

One important parameter in fuel assessment is the lower heating value (LHV), which indicates the heat output during combustion. The LHV of bio-ethanol is 26.9 MJ/kg, which is significantly lower than gasoline's 44 MJ/kg. Consequently, if no adjustments are made to the fuel system, engine efficiency may decline [4]. Another critical factor is the air-to-fuel ratio (A/F), which represents the amount of air required for the complete combustion of one kilogram of fuel. Since bio-

* Corresponding author: Khanh Nguyen Duc.

ethanol contains roughly 34% oxygen by mass, it needs less air for full combustion than gasoline does. While gasoline requires an A/F ratio of 14.6 kg, pure bio-ethanol necessitates only 9.0 kg, allowing a greater volume of ethanol to be burned within the same air intake [5].

Moreover, bio-ethanol has a higher research octane number (RON) compared to gasoline, meaning it exhibits better resistance to detonation combustion. Commercial gasoline generally has a RON between 92 and 98, whereas bio-ethanol reaches a value of 107 [6]. This property enhances the thermal efficiency of S.I. engines, especially in terms of compression ratio optimization. Additionally, bio-ethanol's greater heat of vaporization benefits engines by improving volumetric efficiency and reducing knocking in direct injection S.I. engines [7]. However, this feature also presents challenges in blending bio-ethanol with charged air, as it can decrease the in-cylinder temperature, prolong combustion duration, and lead to higher emissions when used in high concentrations [8].

Bio-ethanol's relatively low Reid vapor pressure (RVP) creates difficulties in cold starts and stable idling conditions [9]. Nonetheless, challenges such as unstable idling and cold-starting difficulties persist due to ethanol's high latent heat of vaporization and lower RVP. The difference between the two types of fuel causes engines using high-ethanol blends to experience issues such as unstable idling, and poor exhaust emissions during the warm-up phase. In the study conducted by Tien et al. [10], a novel intake air heating solution proved to be effective in improving cold start performance of a fuel injection motorcycle. Exhaust emission quality was significantly enhanced during the warm-up phase when the engine operated on ethanol.

To improve engine performance, various modification and adjustment solutions can be considered, such as optimizing the ignition timing (IT), changing the engine's compression ratio, preheating the intake air or fuel injectors, and using fuel additives. In practice, when running a S.I. engine entirely on ethanol, the IT must be advanced. Research by Alfredas [11] has shown that the IT needs to be increased to achieve optimal engine performance. Similar studies, such as the use of compressed natural gas in gasoline engines [11], have also indicated the same trend. With the optimal ignition timing, brake mean effective pressure (BMEP) can improve significantly. However, adjusting IT is a complex solution, especially for retrofitting currently used vehicles. Another potential improvement is charging compression ratio technology. Ethanol's high RON, as previously discussed, makes it highly compatible with higher compression ratios, significantly enhancing thermal efficiency without the risk of knocking. However, altering the compression ratio is structurally complex and affects engine durability and it is impossible to switch back to gasoline.

In addition to these modifications, researchers have explored the role of fuel additives in enhancing combustion efficiency, improving fuel economy, and lowering emissions. For example, dimethyl ether, which has a low boiling point and high vapor pressure, has been utilized in diesel engines to optimize performance [12]. Hydrogen, another additive, has been examined for its potential to accelerate combustion and increase efficiency in natural gas engines [13]. HHO gas, derived from water electrolysis, has also been studied as a fuel additive in both C.I. and S.I. engines. Research indicates that blending HHO with biodiesel-diesel mixtures enhances thermal efficiency, improves power output, lowers fuel consumption, and significantly reduces emissions such as CO, HC, and NO_x [14]. Similarly, applying HHO in gasoline-bioethanol S.I. engines has been found to accelerate combustion but may result in higher NO_x emissions [15].

In Vietnam, integrating ethanol into the transportation sector is a practical approach to lowering fossil fuel consumption and emissions, aligning with the country's sustainability goals. However, research on vehicles operating solely on ethanol or high-ethanol blends remains limited. Some investigations have explored using exhaust heat or electric intake air heating to optimize ethanol-powered engines, but further studies are needed to advance ethanol adoption in the automotive sector. As analyzed above, when using pure ethanol, several issues need to be addressed, such as adjusting the IT, preheating the intake air, or using fuel additives. Implementation of fuel additives is a feasible solution without any significant modification in the currently used vehicle. Therefore, in this study, the research team aims to determine optimal parameters and select suitable solutions for converting existing engines to run entirely on ethanol, that is fuel additive implementation. This study seeks to address ethanol-fueled vehicle challenges by assessing engine performance and combustion characteristics of ethanol-gasoline-fueled engines by simulation. The AVL-Boost simulation software was utilized to examine parameters such as in-cylinder pressure, net rate of heat release (RoHR), ignition delay (ID), and combustion duration (CD), offering deeper insights into ethanol combustion dynamics. The effects of HHO on ethanol-fueled engines are also evaluated. The results of this study serve as a basis for developing solutions to improve the performance of ethanol engines in vehicles currently in use.

2. Material and methodology

2.1. Study procedure

The research process consists of several steps, as illustrated in Figure 1. First, the model is developed based on technical documentation and actual structural parameters. Then, in the next step, the accuracy of the model is evaluated by comparing certain simulated parameters with experimental data. Finally, once the model achieves an acceptable level of accuracy, gasoline is replaced with blends at different high ethanol levels from E50 to E100. For the high ethanol content blends, HHO is used for the improvement of engine performance. The simulation results of the economic and performance of the ethanol-gasoline blends powered engine are then analyzed based on the defined simulation scenarios.

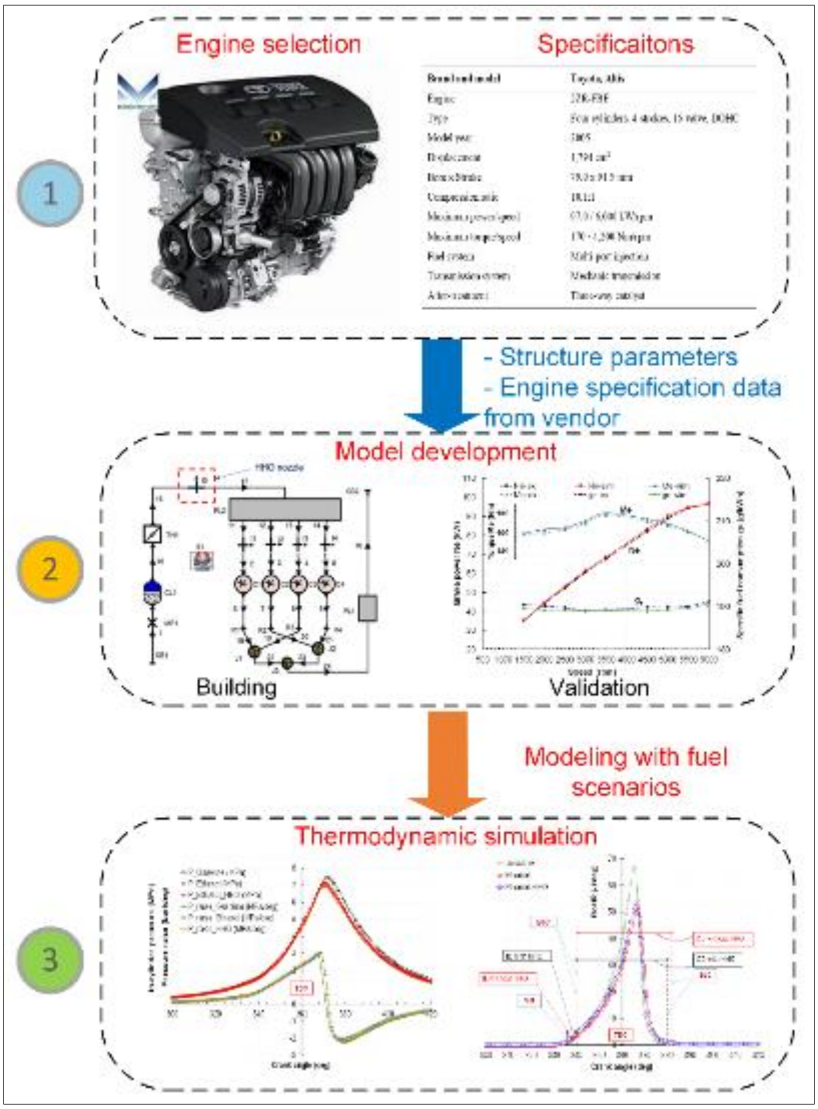

Figure 1 The study procedure flowchart

2.2. Engine specifications

The research in this study was conducted based on a widely used engine, with the primary engine specifications detailed in Table 1.

Table 1 The test engine specifications

Brand and model	Toyota, Altis
Engine	1ZZ-FE
Type	Four cylinders, 4-strokes, 16-valve, DOHC
Model year	2005
Displacement	1,794 cm^3
Bore x Stroke	79.0 x 91.5 mm
Compression ratio	10.1:1
Maximum power/speed	97.0 / 6,000 kW/rpm
Maximum torque/speed	170 / 4,200 Nm/rpm
Fuel system	Multi-port injection
After-treatment	Three-way catalyst

The fuels used in the validation test in this study consisted of commercially available A95 gasoline. Table 2 presents a comparison of the essential properties of ethanol, gasoline, and hydrogen, as referenced from existing literature sources.

Table 2 The critical properties of test fuels

Property	Ethanol	Gasoline	Hydrogen	Reference
RON	107	92–98	130+	[6, 16]
The heat of vaporization (kJ/kg), 1 atm 25°C	900–920	380–400	-	[17]
Carbone content (%w)	52.2	85	0	
Oxygen content (%w)	34.7	0	0	
Density (kg/m^3) at 15°C	785–809.9	750–765	0.0838[a]	[17, 18]
LHV (MJ/kg)	26.9	44.0	119.96	[6, 17, 18]
Air to fuel ratio (kg)	9.0	14.6	34.3	
Laminar flame speed (m/s)	0.39[b]	0.33[b]	2.83[c]	[17, 18]
Auto ignition temperature (°C)	423	230–480	585	[18]
RVP (kPa) at 37.8°C	17.0	53–60	-	[17]
Flammability ranges (%)	3.3–19	1–7.6	4-75	[19, 20]

Note: (a) at 100 kPa and 293K; (b) at 100 kPa and 325K; (c) Maximum flame velocity in air

2.3. Simulation model development

When direct measurement tools are unavailable or the experimental setup is too complex to analyze certain parameters, modeling serves as an alternative approach. In this study, the commercial software AVL Boost was used to develop a simulation model to predict the impact of fuel used on the combustion process and in-cylinder characteristics and engine performance. The constructed model, illustrated in Figure 2, was designed based on the engine’s structural parameters. The simulation applies the first law of thermodynamics to determine the engine’s pressure cycle. The Fractal combustion model [21], wall heat transfer analysis, and gas properties that change with pressure, temperature, and composition are incorporated into the developed model [22].

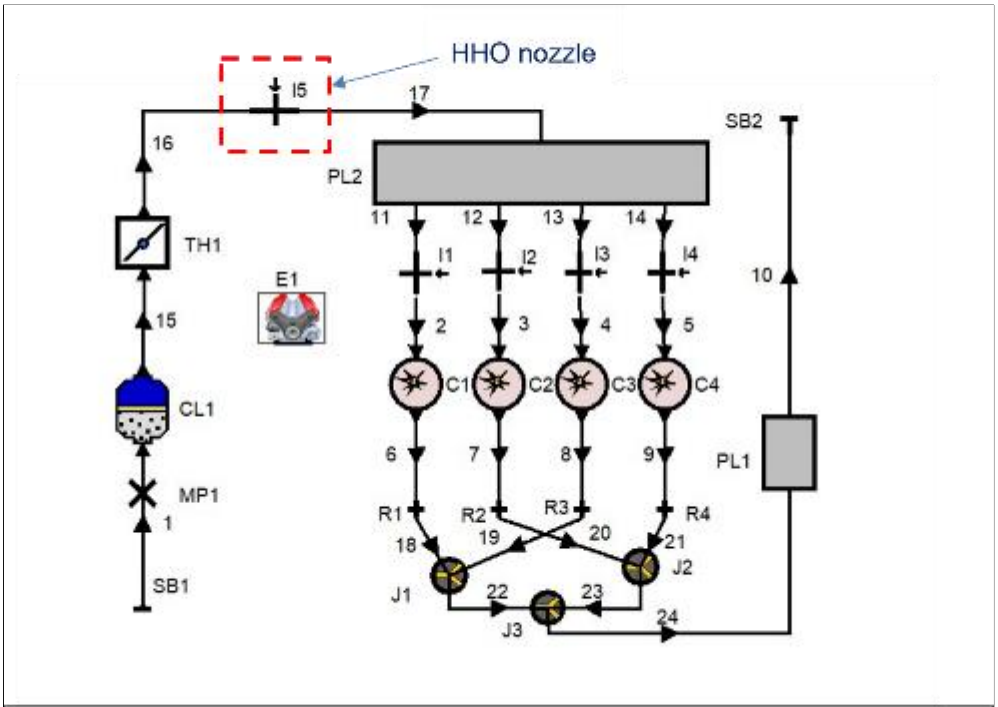

Where SB is system boundary; MP is measuring point; C is cylinder; PL is plenum; CL is air cleaner; TH is throttle; J is junction; R is restrictor; I is injector.

Figure 2 Developed model of the 1ZZ-FE engine

2.4. Simulation Scenario

First, the model was run using gasoline under wide-opened throttle (WOT) conditions as a baseline to evaluate the model's reliability by comparing power output, torque, and fuel consumption data between the simulation results and the manufacturer's specifications. Once the model demonstrated acceptable accuracy, with deviations in specific fuel consumption and power/torque output being less than 5%, gasoline was then replaced with ethanol-gasoline blends containing 50%, 70%, 85%, and 100% ethanol, respectively.

For each of the four ethanol-gasoline blend cases, the simulation was further refined by introducing HHO as a fuel additive at a volumetric ratio of 0.1% relative to intake air. This was treated as an additive to enhance combustion when the engine operates on biofuels. The simulation was conducted at a mid-range engine speed of 4200 rpm, which corresponds to optimal engine performance. Parameters such as brake mean effective pressure (BMEP), indicated mean effective pressure (IMEP), in-cylinder pressure (P), temperature (T), heat release rate (RoHR), mass fraction burned (MFB), and pressure rise were analyzed and evaluated.

3. Results and discussion

3.1. Validation of simulation models

Figure 3 presents the IMEP and BMEP values across simulated cycles under rated operation at 4200 rpm with WOT. It can be seen that both the IMEP and BMEP graphs share a similar overall trend: the initial values fluctuate significantly during the first few cycles, then quickly decrease to a stable value. The calculated mean absolute error (MAE) is less than 0.274 bar after 20 iterations for IMEP and BMEP. This confirms that the simulation data have converged, making them suitable for further comparative studies.

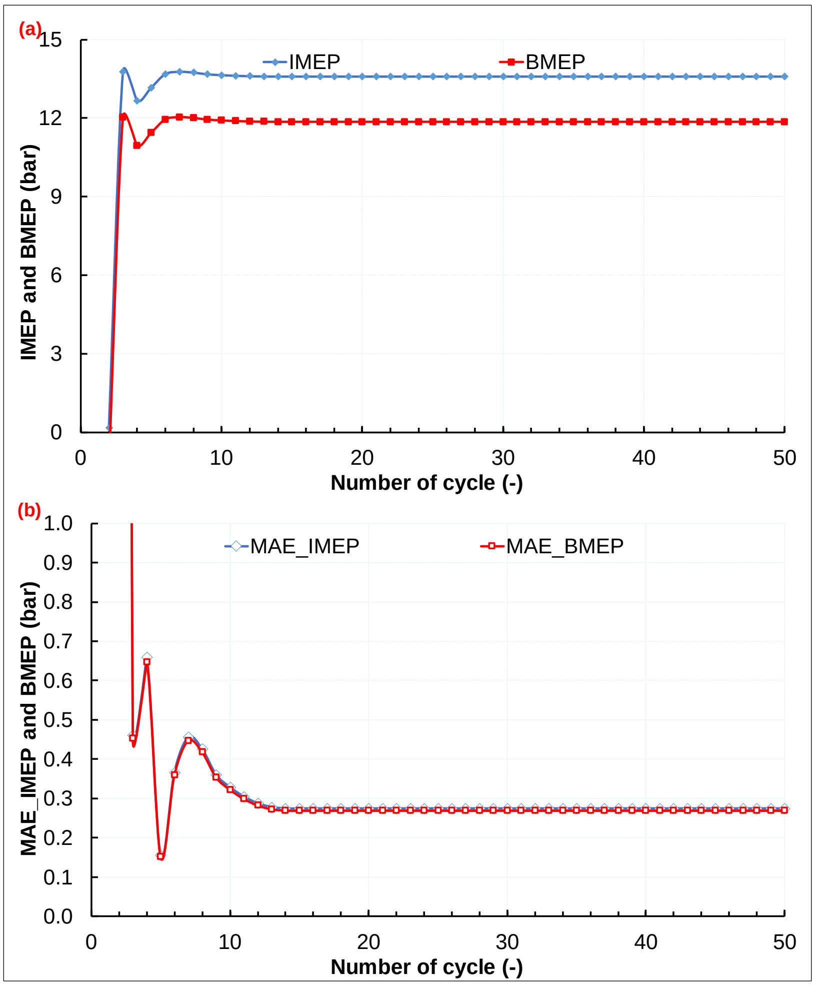

Figure 3 The simulated (a) IMEP and BMEP and (b) MAE as a function of cycles at WOT and an engine speed of 4200 rpm

To ensure accuracy, the simulation model was validated by comparing its outcomes with data supplied by the vendor under varying engine operating conditions, as shown in Figure 4. The results indicate that the trends in brake power and brake-specific fuel consumption (BSFC) from the simulation closely match those observed in the experiment at full load. This demonstrates strong consistency between both datasets. The difference between simulated and experimental brake power and BSFC values averaged deviation is 3.1% across the entire simulated speed range, with the maximum deviation reaching 4.6%. Minor discrepancies arise due to certain assumptions made in the simulation that cannot be precisely controlled in practical tests. However, these variations are minimal, confirming the reliability of the simulation model for further combustion studies.

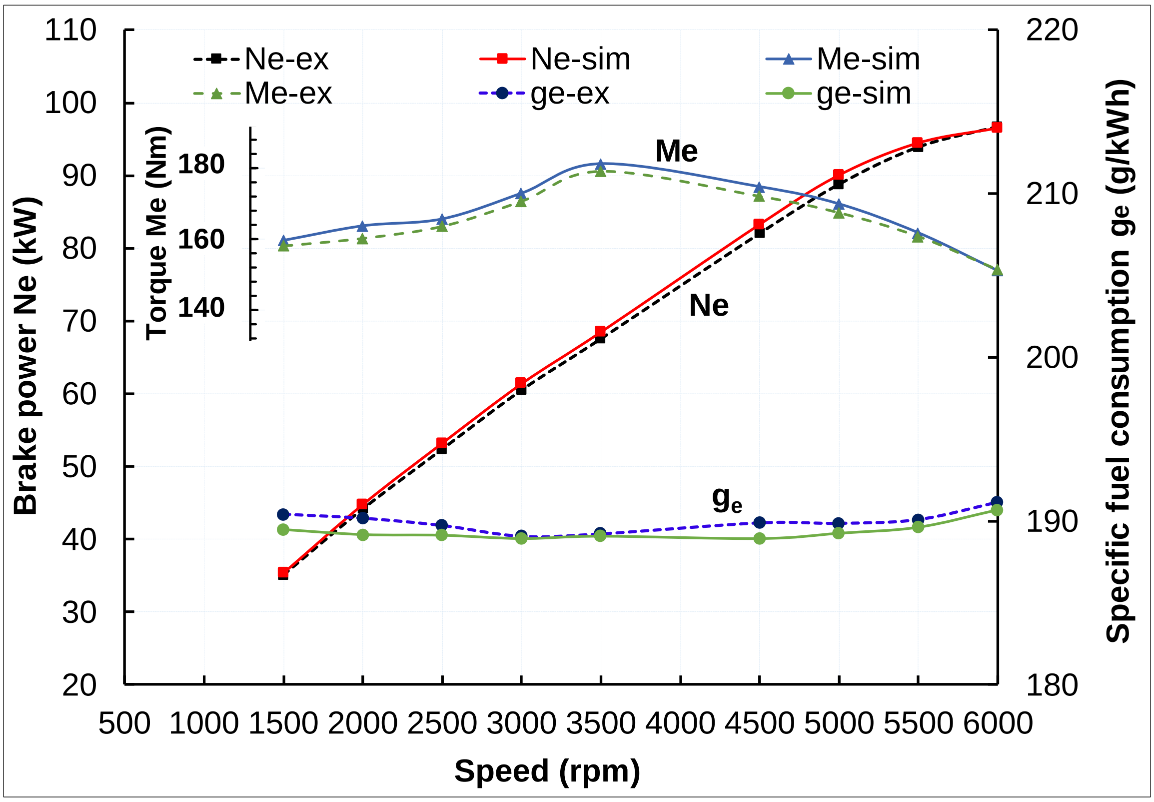

Figure 4 Comparison of brake power, torque, and specific fuel consumption at WOT conditions

3.2. The effects of ethanol proportion on the combustion process

The simulation results of in-cylinder pressure at 4200 rpm under WOT conditions are illustrated in Figure 5. It is clearly observed that when using 100% ethanol, the peak in-cylinder pressure was remarkable decreased around the top dead center (TDC), from 7.474 bar to 7.326 bar. This reduction is reasonable due to the substantial differences in the physical and chemical properties between gasoline and ethanol, particularly ethanol's high latent heat of vaporization and higher RON. These factors influence the combustion process, while other engine parameters such as compression ratio and IT remain unchanged, originally optimized for gasoline operation. However, as the ethanol content in the fuel blend was gradually reduced in the blends, the in-cylinder pressure tended to increase - reaching approximately 7.393 bar with E85 and 7.375 bar with E70. Notably, when the engine operates with E50, the peak in-cylinder pressure was raised significantly to 7.560 bar, exceedingly even the peak pressure observed with pure gasoline.

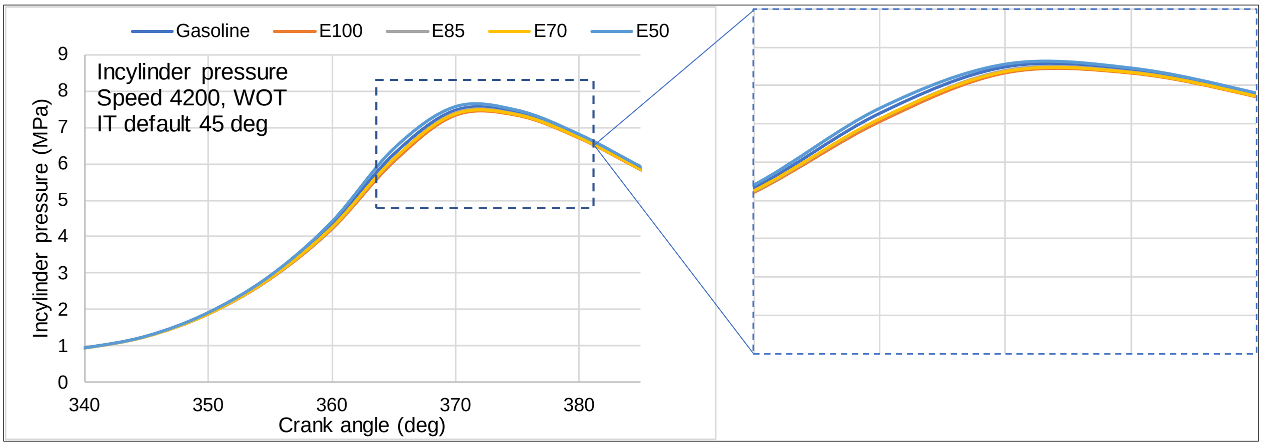

Figure 5 In-cylinder pressure profiles with different fuel blends

Figure 6 illustrates the variation of the net RoHR for fuel samples with varying ethanol content. It can be observed that when using E100 fuel, the peak RoHR tended to decrease to approximately 64.09 J/deg from 66.44 J/deg for gasoline, and the combustion process became significantly prolonged as compared to gasoline. Similar trends were observed with E85 and E70, where the maximum RoHR reached 64.89 J/deg and 63.64 J/deg, respectively. However, this trend reversed when the engine was operated with E50 fuel. In this case, the RoHR was increased, and combustion occurred earlier, with the peak RoHR reaching 66.12 J/deg. This indicates that using an ethanol-gasoline blend with 50% ethanol or less may theoretically improve the combustion process, especially in terms of heat release characteristics. Nevertheless, in practical applications, many other influencing factors that are not fully addressed in the simulation-such as mixture formation, turbulence intensity, heat losses, and real ignition behavior slightly alter this conclusion. Therefore, while the simulation provides valuable theoretical insights, experimental validation is essential to confirm the actual impact under real engine operating conditions.

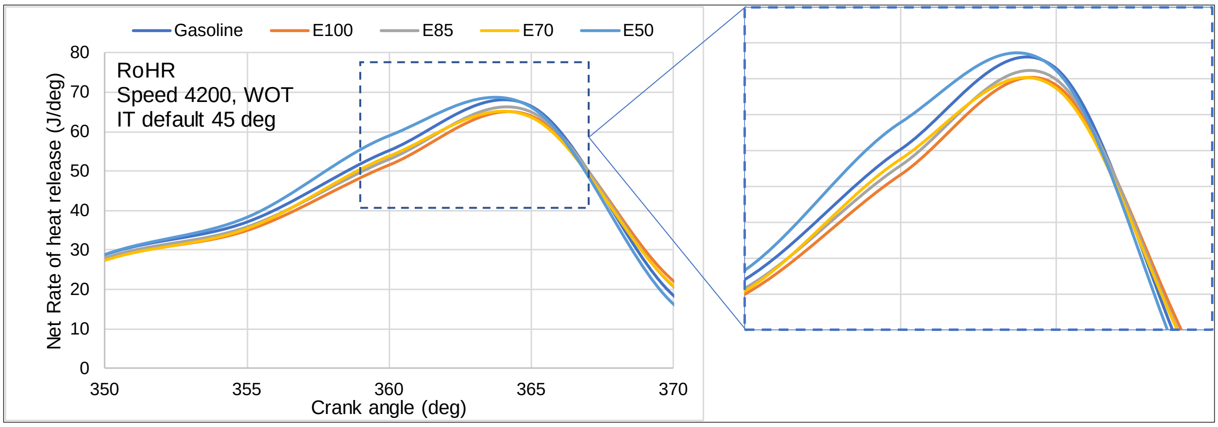

Figure 6 Net rate of heat release profiles with different fuel blends

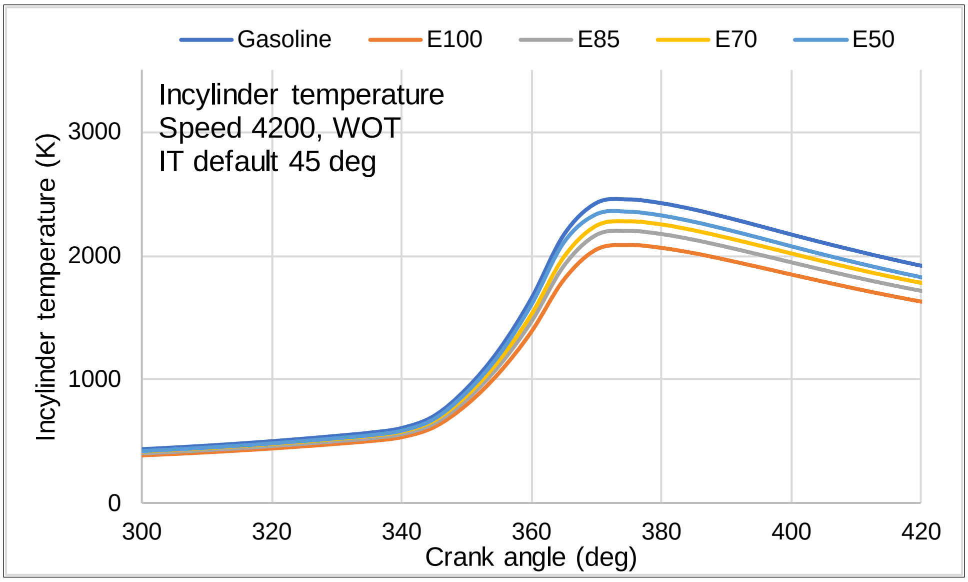

Figure 7 In-cylinder temperature profiles with different fuel blends

Figure 7 illustrates the variation of in-cylinder temperature as a function of crank angle when using different fuel types, including gasoline, E50, E70, E85, and E100. The data were recorded at an engine speed of 4200 rpm, under WOT conditions, and with a fixed IT of 45 degrees before BTDC. From the graph, it is evident that the in-cylinder temperature increased gradually from approximately 345 to 360 degrees crank angle, with the most significant differences observed around the TDC. While the temperature variations between fuel types are not drastic, gasoline generally tends to produce slightly higher peak combustion temperatures compared to bioethanol-based fuel blends. In general, fuels with higher ethanol content, such as E85 and E100, exhibited slightly lower peak temperatures than pure gasoline due to some differences in fuel characteristics such as ethanol's higher latent heat of vaporization and lower energy density. In turn, peak temperatures were 2090K, 2199K, and 2277K for E100, E85, and E70, respectively. Notably, when operating with E50, the in-cylinder temperature tended to be higher than that of other ethanol-gasoline blends, with the peak temperature reaching approximately 2354K, compared to 2450K when using pure gasoline. This suggests that E50 may offer a thermally favorable combustion profile under the given operating conditions.

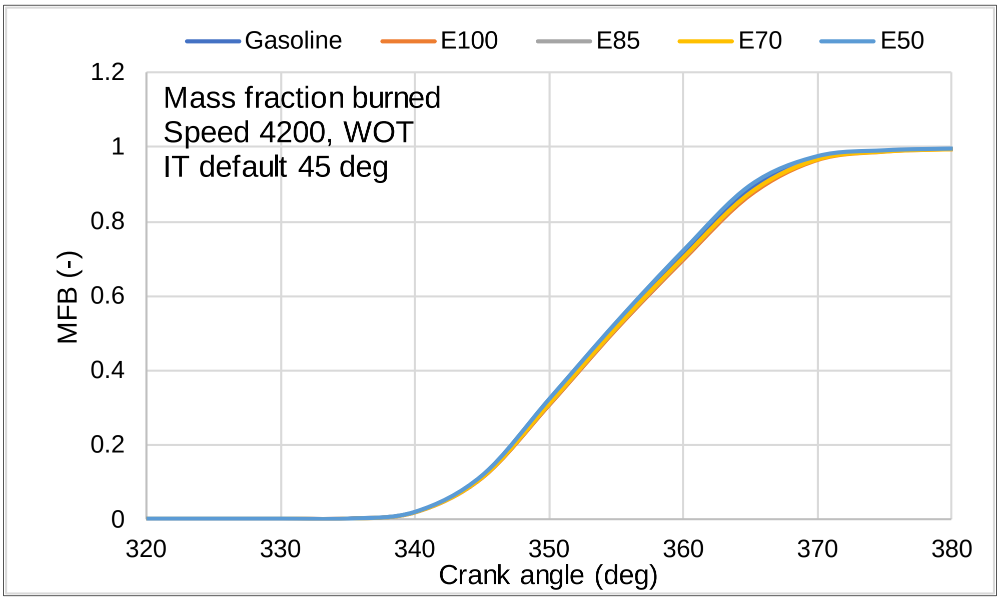

Figure 8 Mass fraction burned profiles with different fuel blends

The MFB graph plotted against the crank angle in Figure 8 illustrates the combustion process of various fuels - gasoline, E50, E70, E85, and E100. According to the graph, combustion generally begins around 325–330 degrees crank angle and completes shortly after the TDC, approximately at 360 degrees. Although all fuel types follow a similar combustion duration, there are subtle differences in the combustion rate. In particular, fuels with higher ethanol content, such as E85 and E100, exhibit slower combustion rates, as indicated by the gentler slope of the MFB curve compared to traditional gasoline. This slower burn is primarily attributed to ethanol's higher latent heat of vaporization and distinct combustion characteristics, which influence flame propagation and delay the heat release process.

3.3. The effect of HHO on the combustion process of engines fueled by different ethanol-gasoline blends

The graph illustrates the in-cylinder pressure variation with a crank angle for different ethanol-based fuels (E50, E70, E85, E100), comparing two scenarios: using gasoline-ethanol fuel blends with and without HHO. The simulation condition was similar, at an engine speed of 4200 rpm, WOT, and a default IT of 45 degrees. As a result, no modifications were made to optimize combustion - only the fuel type was changed. This approach is beneficial for retrofitting existing vehicles, as evidenced by Duy et al. (2020), where Maz additives were used in a converted natural gas engine originally designed for gasoline [23]. The HHO additive was introduced at a consistent 0.1% airflow rate, aligning with previous research [12, 23].

Observations show that the addition of HHO consistently increased the peak in-cylinder pressure across all ethanol concentrations. Specifically, the pressure curves for the HHO-assisted cases were slightly higher and reached their peak earlier compared to the non-HHO cases. This phenomenon is attributed to the high flammability and rapid flame propagation characteristics of HHO gas. When introduced into the combustion chamber, HHO acts as a combustion enhancer, accelerating the burn rate and making the combustion process more efficient. The faster combustion leads to higher pressure near the TDC, thereby improving the engine's indicated thermal efficiency. Additionally, HHO helps shorten the combustion duration, reduce heat losses, and potentially lower emissions of harmful pollutants such as CO and HC due to more complete combustion.

Based on the graph in Figure 9, it is evident that the effect of HHO varies depending on the ethanol content. The impact was most pronounced with E100, where the difference in pressure curves with and without HHO was significant; peak pressure was notably higher and occurred earlier. In contrast, with E50, the pressure curves nearly overlapped, indicating minimal influence of HHO on combustion characteristics. This suggests that the HHO additive effect becomes more effective at higher ethanol concentrations, likely due to its role in enhancing combustion in fuels with less gasoline content.

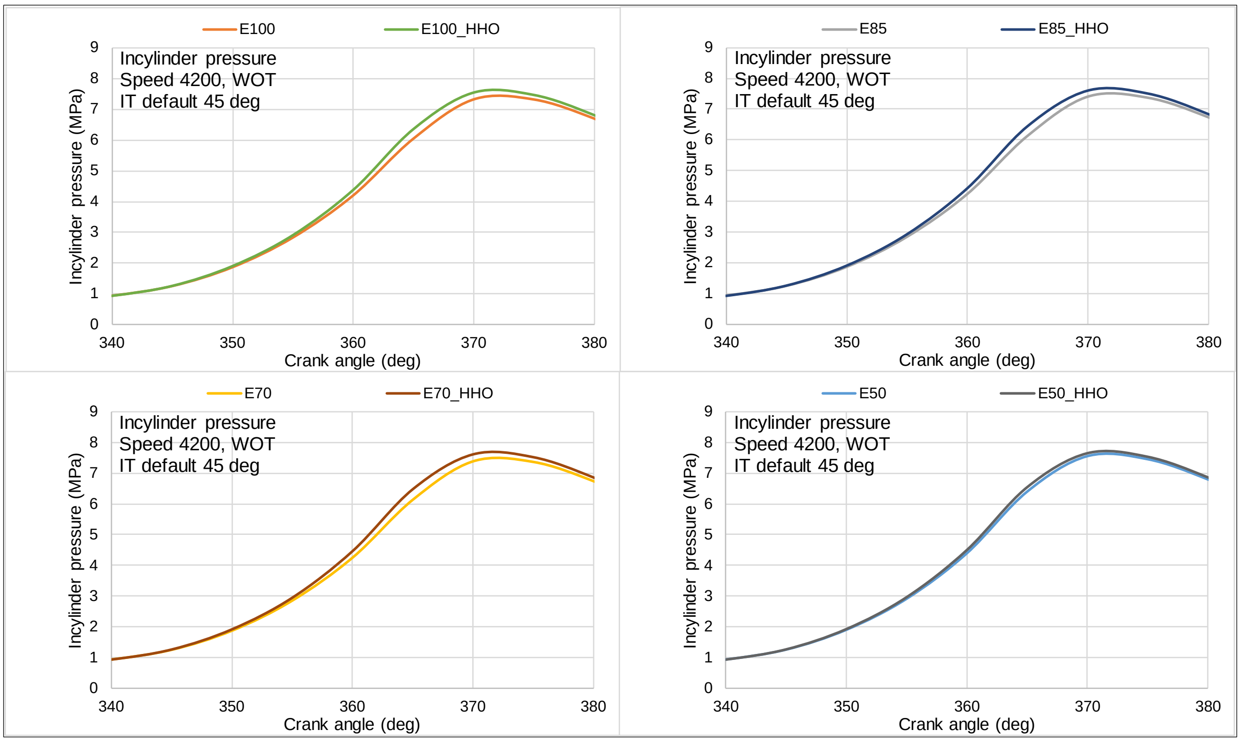

Figure 9 The effect of HHO on in-cylinder pressure with different fuel blends

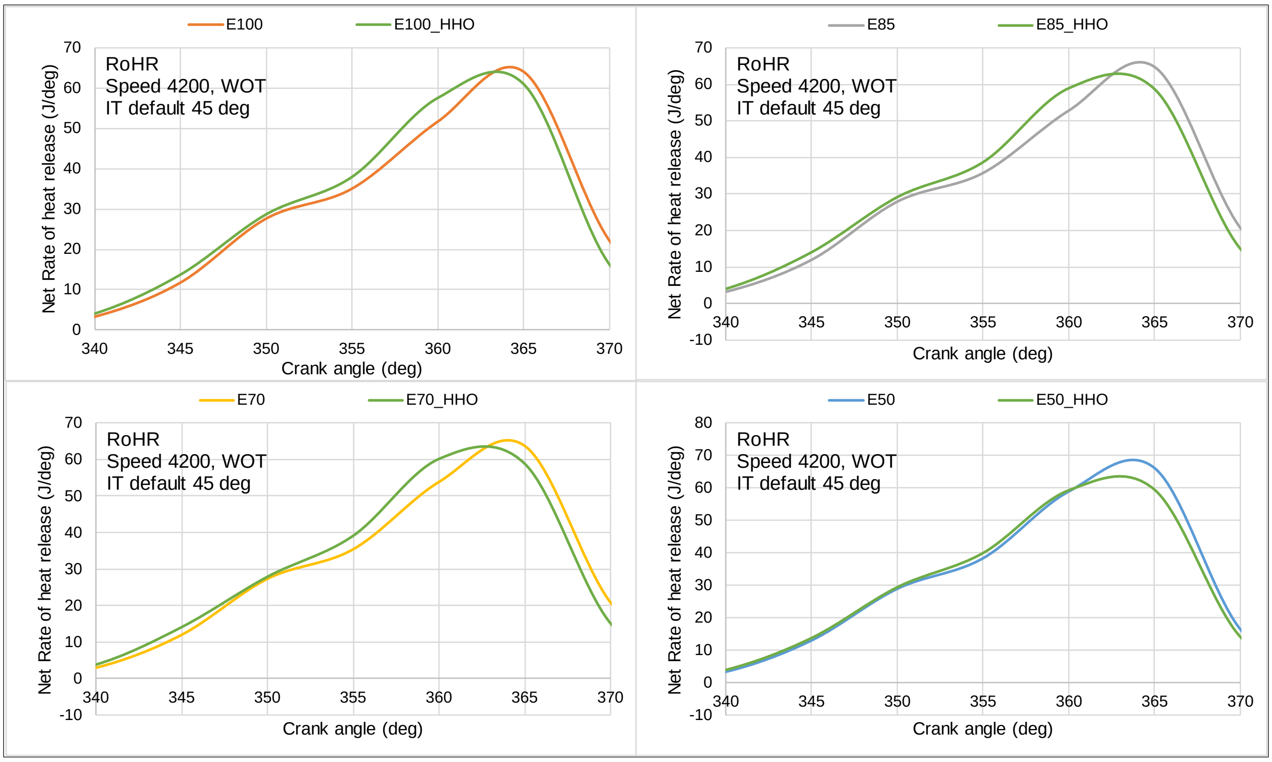

Figure 10 The effects of HHO on net RoHR with different fuel blends

As seen in Figure 10, it is evident that HHO has a significant impact on increasing the RoHR, especially during the early combustion phase, clearly seen around the TDC. For high-ethanol fuels such as E100 and E85, the RoHR curve with HHO (green line) was raised sharply compared to the non-HHO case, with a noticeably higher and earlier peak. This indicates that the combustion process becomes more intense and rapid, owing to the combustion-enhancing characteristics of HHO, which include fast ignition and high flame propagation thereby accelerating the heat release rate [15]. In contrast, for E70 and particularly E50, the influence of HHO is much less pronounced. In the E50 case, the RoHR curves with and without HHO are nearly overlapping after igniting at the crank angle of 45 degrees before the TDC, suggesting that HHO has minimal effect on combustion characteristics at lower ethanol concentrations. This aligns with the inherently higher flammability of the E50 blend, which reduces the relative contribution of HHO in promoting combustion.

In summary, the effect of HHO on RoHR was most significant for E100 and diminished progressively toward E50. This suggests that HHO is more effective when used with fuels containing higher ethanol content, where it can enhance combustion speed, improve thermal efficiency, and increase the engine's power output potential.

3.4. Deep analysis of the effect of HHO on the combustion process of the engine fueled by pure ethanol

Figure 11 displays the simulated results for engine combustion at WOT and a fixed speed of 4200 rpm. The lambda ratio was set at a stoichiometric level of 1.0 for both gasoline and bio-ethanol, while IT remained unchanged from the gasoline default.

A slight increase in BMEP was noted, with values rising by 5.05% for bio-ethanol and 6.06% for bio-ethanol-HHO (0.99 MPa for gasoline, 1.04 MPa for ethanol, and 1.05 MPa for ethanol-HHO). Meanwhile, BSEC exhibited a decline of 7.70% from 19.62 MJ/kWh to 18.11 MJ/kWh for bio-ethanol and 10.65% to 17.53 MJ/kWh for bio-ethanol-HHO. These trends align with findings by Sami et al. [24], reinforcing that ethanol fuel enhances the engine's efficiency without requiring further modifications to combustion parameters. Additionally, these results correspond well with experimental observations reported by Lee et al. [25].

To maintain engine power, the ethanol supply was adjusted to match the stoichiometric air-fuel ratio. As shown in Figure 11, the graph presents normalized values for BMEP and brake-specific energy consumption (BSEC) when utilizing ethanol and ethanol-HHO relative to gasoline.

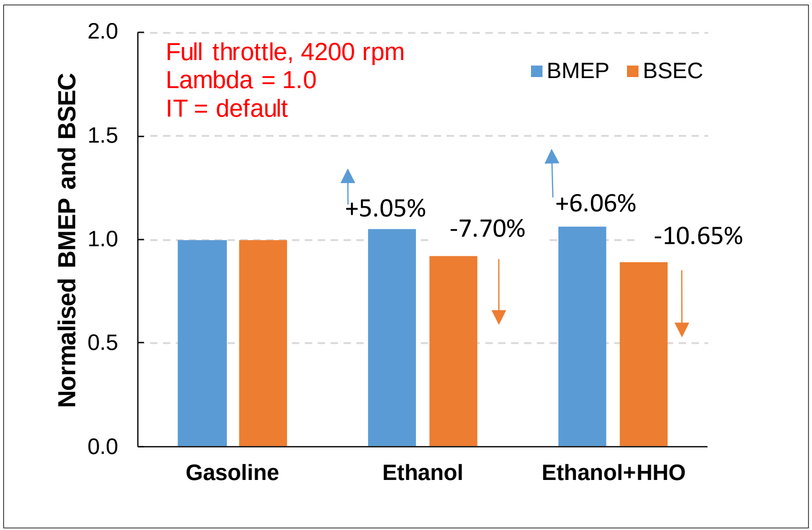

Figure 11 Comparison of BMEP and BSEC with different fuels

Figures 12 and 13 compare the in-cylinder pressure and temperature profiles for various fuel types scenarios: gasoline, and pure ethanol (E100) with and without HHO. Engines running on bio-ethanol display lower peak cylinder pressures than those using gasoline. This reduction is mainly due to ethanol's higher RON, which delays ignition, and its substantial latent heat of vaporization, which slows down both ignition and heat release, as previously noted by Qian et al. [26]. For example, at a crank angle of 371 degrees, the ethanol-fueled engine without HHO enhancement reached a peak pressure of 6.98 MPa, while the gasoline-fueled engine attained a higher pressure of 7.49 MPa at 372 degrees. When HHO was introduced alongside ethanol, the peak pressure rose to 7.16 MPa at the same crank angle, suggesting that HHO improves the combustion process by advancing the ignition and increasing completeness. These findings align with earlier research indicating that hydrogen or hydrogen-containing additives enhance S.I. engine combustion [27, 28].

AVL Boost simulation results show that pressure rise rates varied with fuel types. With gasoline, the maximum pressure rise was 3.01 bar/deg, while ethanol recorded 2.89 bar/deg. This value increased slightly to 2.92 bar/deg when ethanol was combined with HHO (Figure 12). Ethanol combustion also produced lower peak temperatures due to its high latent heat. The in-cylinder temperature dropped from 2448.7 K (gasoline at 375° CA) to 2025.5 K (ethanol at 373° CA). Adding HHO raised the peak temperature slightly to 2123.4 K at the same crank angle, indicating a modest improvement in combustion (Figure 13).

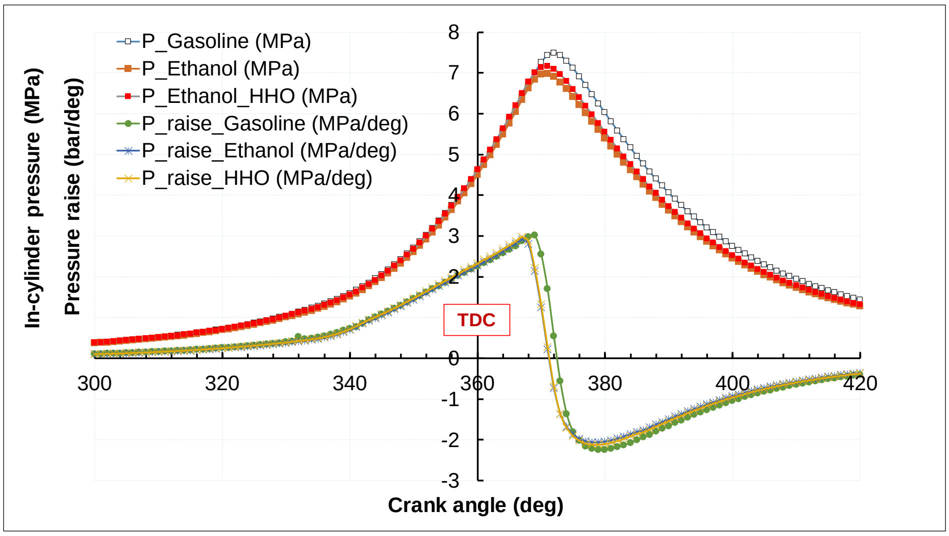

Figure 12 In-cylinder pressure with different fuels

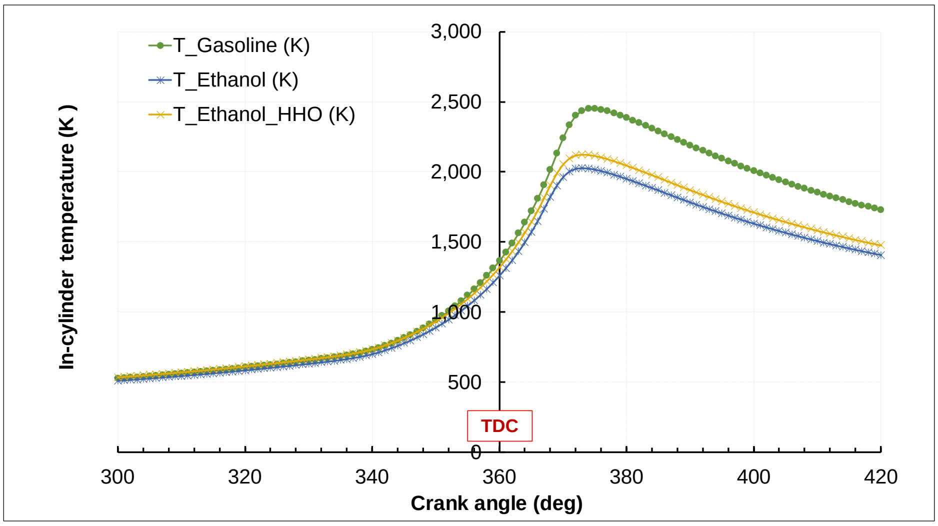

Figure 13 In-cylinder temperature with different fuels

Figure 14 presents a comparative analysis of key combustion parameters, including net RoHR profiles, ID, and CD, under full-load conditions at an engine speed of 4200 rpm. Near the TDC, a clear difference is observed between gasoline and ethanol-fueled cases in terms of RoHR magnitude. Gasoline achieves a peak RoHR of 66.69 J/deg, while pure bio-ethanol reaches a lower peak of 52.84 J/deg. When HHO is introduced, the ethanol-fueled engine records a slightly higher peak RoHR of 53.46 J/deg at a crank angle of 367 degrees.

The ignition delay (ID) is defined as the interval from the start of ignition (SoI) to the beginning of combustion (BoC), whereas the combustion duration (CD) corresponds to the time required to reach 95% mass fraction burned from BoC to the end of combustion (EoC). Ethanol-fueled cases show a longer CD compared to gasoline, due to ethanol's slower combustion characteristics. However, with the addition of HHO, ID is slightly reduced at the same SoI, attributed to improved charge mixture uniformity. The presence of HHO also leads to a decrease in CD - from 41.5 degrees in the ethanol-only case to 40.0 degrees in the ethanol with HHO configuration. These observations are consistent with findings from previous studies by Alfredas et al. [15], Amrouche et al. [29], and Akçay & Gürbüz (2024) [30], which have shown that hydrogen enrichment promotes faster combustion, enhances thermal efficiency and reduces brake-specific energy consumption.

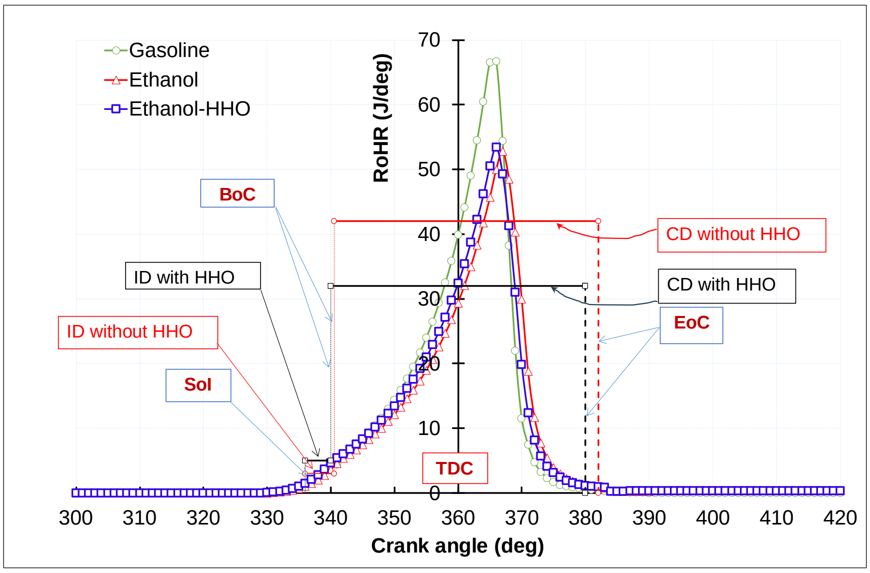

Figure 14 Net of the rate of heat release with different fuels

As previously discussed, although the total energy input to the engine remains nearly the same when operating on either gasoline or ethanol at a constant lambda ratio, differences in fuel characteristics significantly influence combustion behavior. Since IT was not adjusted in the simulation, these differences led to delayed peak in-cylinder pressure during ethanol operation. This highlights the need for IT optimization when using ethanol in order to maximize combustion efficiency, as noted in [15]. However, adjusting IT in existing engine systems typically involves complex modifications to control systems or hardware. Consequently, this study retained the original IT configuration. Instead, the introduction of HHO was proposed as an alternative approach to partially enhance combustion performance without requiring major changes to engine control or calibration.

Nomenclature

CO	Carbone monoxide
NO_x	Nitrogen oxide
HC	Hydrocarbons
A/F	Air-to-fuel ratio

Abbreviation

S.I.	Spark ignition engine
LHV	Lower heating value
RON	Research octane number
RVP	Reid vapor pressure
HHO	Oxy-hydrogen
RoHR	Rate of heat release
ID	Ignition delay
IT	Ignition timing
IMEP	Indicated means effective pressure
CD	Combustion duration

C.I.	Compress ignition engine
DOHC	Double overhead camshaft
MAE	Mean absolute error
MFB	Mass Fraction Burned
BMEP	Brake means effective pressure
BSEC	Brake-specific energy consumption
BSFC	Brake-specific fuel consumption
SoI	Start of ignition
SoC	Start of combustion
EoC	End of combustion
TDC	Top dead center
WOT	Wide opened throttle

4. Conclusion

The simulation study of the combustion process in a spark-ignition engine using high-percentage ethanol-gasoline blends was conducted using the advanced simulation tool AVL-Boost. The key findings of the study include:

- Fuels with a high ethanol content have a significant impact on the combustion process, as evidenced by reductions in peak in-cylinder pressure, temperature, and heat release rate. Additionally, the combustion duration is extended, and the level of impact increases progressively with the ethanol ratio in the blends.
- In contrast, the fuel blend with a lower ethanol content, specifically E50, showed improved combustion performance, as in-cylinder parameters tended to increase.
- The presence of HHO in the intake air, acting as an additive, demonstrated a positive effect on enhancing the combustion process. The degree of improvement became more significant with higher ethanol content in the fuel blend.
- Conversely, for the medium ethanol blend (E50), the addition of HHO had little to no observable effect. This is likely because, at this ethanol-gasoline ratio, the combustion process had already been optimized.

Compliance with ethical standards

Disclosure of conflict of interest

No conflict of interest to be disclosed.

References

[1] Saikrishnan, V., Karthikeyan, A., & Jayaprabakar, J. Analysis of ethanol blends on spark ignition engines. Int. J. Ambient Energy 39(2) (2018) 103-107. doi: 10.1080/01430750.2016.1269678

[2] Kathirvel, S., Apurba, L., & Muthuraman, S. Performance characteristics of CI engine using blends of waste cooking oil methyl ester, ethanol and diesel. Int. J. Ambient Energy 41(5) (2018) 570-581. doi: 10.1080/01430750.2018.1477061

[3] Iodice, P., Langella, G., Amoresano, A. Ethanol in gasoline fuel blends: Effect on fuel consumption and engine out emissions of SI engines in cold operating conditions. Appl. Therm. Eng 130 (2018) 1081-1089. doi: 10.1016/j.applthermaleng.2017.11.090

[4] Thanh, D., Khanh, N., Tuan, P. & Vinh, N. Study on performance enhancement and emission reduction of used carburetor motorcycles fueled by flex-fuel gasoline-ethanol blends. J. Chin. Inst. Eng 43(5) (2020) 477-488. doi: 10.1080/02533839.2020.1751719

[5] Mohammed, M. K., Balla, H. H., Al-Dulaimi, Z. M. H., Kareem, Z. S., & Al-Zuhairy, M. S. Effect of ethanol-gasoline blends on SI engine performance and emissions. Case Stud. Therm. Eng 25 (2021) 100891. doi: 10.1016/j.csite.2021.100891

[6] Abdulfatah, A.Y., and Freddie L.I. Progress in alcohol-gasoline blends and their effects on the performance and emissions in SI engines under different operating conditions. Int. J. Ambient Energy 42(4) (2021) 465-481. doi: 10.1080/01430750.2018.1531261

[7] Li, X., Xie, F., Liu, Y., Li, X., Su, Y., & Zhou, Y. Study on the Influence of Different Internal Exhaust Gas Recirculation Formation Modes on the Combustion Performance of Gasoline, Methanol, and Ethanol SI Engine. Int.J Automot. Technol 25 (2024) 495–505. doi: 10.1007/s12239-024-00039-1

[8] 8. Wang, C., Zeraati-Rezaei, S., Xiang, L., Xu, H. Ethanol blends in spark ignition engines: RON, octane-added value, cooling effect, compression ratio, and potential engine efficiency gain. Appl. Energy 191 (2017) 603–619. doi:10.1016/j.apenergy.2017.01.081

[9] Ansari, A.M., Memon, L.A., Solangi, F.A., Mamdouh T. G., Mohamed Y.E.S. Influence of alcohol blend fuels on performance and noise emission in spark ignition engine. Int. J. Thermofluids 26 (2025) 101120. doi:10.1016/j.ijft.2025.101120

[10] Tien, N.D, Yen-Lien T. N, Truc, N.T, Khanh, N.D, Vinh, N.D & Toan, N.D. Performance and emission of a converted bio-fuel motorcycle engine in cold condition: A case study. Energy Source., Part A: Recov. Utiliz. Environ. Effect. 45(1) (2023) 3056-3069. doi: 10.1080/15567036.2023.2191063

[11] Alfredas, R., Gabrielius, M., Jonas, M. The influence of hydrogen and oxygen (HHO) gas on engine characteristics under the effect of the lean mixtures of gasoline and bioethanol. Int. J. Hydrogen Energy 48 (99) (2023) 39612-39624. doi:10.1016/j.ijhydene.2023.07.167.

[12] Doan, N.C, Khanh, N.D & Vinh, N.D. Performance and pollutant characteristics of an old generation diesel engine fuelled with dual-fuel diesel-dimethyl ether. Int. J. Ambient Energy 44(1) (2023) 555-563. doi: 10.1080/01430750.2022.2137580

[13] Alrazen, H. A., & Ahmad, K. A. HCNG fueled spark-ignition (SI) engine with its effects on performance and emissions. Renewable Sustainable Energy Rev 82 (2018) 324–342. doi:10.1016/j.rser.2017.09.035

[14] Babu, J.M., Sunil Kumar, K., Ramesh Kumar R.,et al. Production of HHO gas in the water-electrolysis unit and the influences of its introduction to CI engine along with diesel-biodiesel blends at varying injection pressures. Int. J. Hydrogen Energy 52 (2024) 865-885: doi:10.1016/j.ijhydene.2023.06.078.

[15] Alfredas, R., Gabrielius, M., Jonas, M. The influence of hydrogen and oxygen (HHO) gas on engine characteristics under the effect of the lean mixtures of gasoline and bioethanol. Int. J. Hydrogen Energy 48 (99) (2023) 39612-39624. doi:10.1016/j.ijhydene.2023.07.167.

[16] Eere energy. (2001). Hydrogen properties. Retrieved from https://www1.eere.energy.gov/hydrogenandfuelcells/tech_validation/pdfs/fcm01r0.pdf. [Accessed March 26, 2024]

[17] Thakur, A. K., Kaviti, A. K., Mehra, R., & Mer, K. K. S. Progress in performance analysis of ethanol-gasoline blends on SI engine. Renewable Sustainable Energy Rev 69 (2017) 324–340. doi:10.1016/j.rser.2016.11.056

[18] https://h2tools.org/hyarc/hydrogen-data/comparative-properties-hydrogen-and-other-fuels [Accessed March 26, 2024]

[19] The Engineering ToolBox (2003). Gases - Explosion and Flammability Concentration Limits. [online] Available at: https://www.engineeringtoolbox.com/explosive-concentration-limits-d_423.html [Accessed March 26, 2024].

[20] https://www1.eere.energy.gov/hydrogenandfuelcells/tech_validation/pdfs/fcm01r0.pdf [Accessed March 26, 2024]

[21] AVL. AVL Boost Combustion Model. Boost user's guide. Austria; 2011.

[22] AVL. Thermodynamic cycle simulation Boost. Version 3.2. Boost user's guide. Austria; 2011.

[23] Duy, V., Duc, K., Thanh, T.N., Dinh, L., & Anh, T.L. Implementation of fuel additive MAZ 100 for performance enhancement of compressed natural gas engine converted from in-used gasoline engine. J Air Waste Manag. Assoc. 70(9) (2020) 932-943. doi: 10.1080/10962247.2020.1781709

[24] Sami, M.M.E.A, Carlos, R.P.B, José, R.S. Hydrogen addition to ethanol-fuelled engine in lean operation to improve fuel conversion efficiency and emissions. Int. J. Hydrogen Energy 49 (2024) 744-752. doi:10.1016/j.ijhydene.2023.09.048.

[25] Lee, C.S., Huu, T.P., Anh, T.L., Minh, T.P., The, L.N., Duy, T.N., Duc, K.N. Experimental study on the effects of ethanol blends on the combustion process, power performance and emission reduction of a motorcycle spark-ignition engine. Int. J. Ambient Energy 43 (1) (2022) 7150-7160. doi: 10.1080/01430750.2022.2063383

[26] Qian, Y., Liu, G., Guo, J., Zhang, Y., Zhu, L., and Lu, X. Engine Performance and Octane on Demand Studies of a Dual Fuel Spark Ignition Engine with Ethanol/Gasoline Surrogates as Fuel. Energy Convers. Manage. 183 (2019) 296–306. doi:10.1016/j.enconman.2019.01.01.

[27] Truong, N.P., Duc, K.N., Phong, T.X., Nghia, N.T. The effects of HHO-enriched air on the combustion process and emission variation of simulated-biogas fueled spark ignition engine. Int. J. Thermofluids 26 (2025) 101146. doi:10.1016/j.ijft.2025.101146

[28] Purayil, S.T.P., Al-Omari, SAB, Elnajjar, E. Effect of hydrogen blending on the combustion performance, emission, and cycle-to-cycle variation characteristics of a single-cylinder GDI spark ignition dual-fuel engine. Int. J. Thermofluids 20 (2023) 100403. doi:10.1016/j.ijft.2023.100403

[29] Amrouche, F., Erickson, P.A., Varnhagen, S., & Park, J.W. An experimental study of a hydrogen-enriched ethanol fueled Wankel rotary engine at ultra lean and full load conditions. Energy Convers. Manage. 123 (2016) 174–184. doi:10.1016/j.enconman.2016.06.034

[30] Akçay, H., Gürbüz, H. Investigation of the effect of HHO-assisted flame-jet ignition on in-cylinder combustion, engine performance, and environmental indicators in a propane-fueled SI engine. Applied Thermal Engineering 253 (2024) 123730. doi:10.1016/j.applthermaleng.2024.123730.